UDK 536.7:66.017:637.133.3:621.039.534
Original scientific article/Izvirni znanstveni članek

ISSN 1580-2949
MTAEC9, 55(6)763(2021)

# SUPERVISED TUNING OF A CHILLER WITH A COLD PHASE-CHANGE MATERIAL USING AN RSM-SMITH PREDICTOR

# NADZOROVANO UGLAŠEVANJE HLADILA S HLADNO FAZNO SPREMEMBO MATERIALA IN UPORABO SMITHOVEGA RSM NAPOVEDNIKA

**Saranya Subbiah Natarajan[1]*, Thirumarimurugan Marimuthu[2]**

[1]Research scholar, Department of Chemical Engineering, Coimbatore Institute of Technology, Coimbatore, India
[2]Professor and Head, Department of Chemical Engineering, Coimbatore Institute of Technology, Coimbatore, India

*Prejem rokopisa – received: 2021-08-19; sprejem za objavo – accepted for publication: 2021-09-03*

doi:10.17222/mit.2021.235

The proposed work is focused on the tuning of the latent-heat storage of a PCM with MWCNT encapsulation for a chiller system in the milk-pasteurization process using an RSM-based predictive Smith controller. The PCM was synthesized using sodium polyacrylate and MWCNT particles, encapsulated in spherical balls stored in the IBT (ice bank tank of the chiller unit). Experimental work is conducted on the heat-transfer characteristics of the chiller unit with servo-operated flow-control valves based on the central composite design of experiments. The system is cascaded using a PID controller with a Smith predictor to stabilize the latent temperature of milk cooling in the chiller system. The system is considered to be a first-order transformation with the rise and settling time. The plant model is obtained, using the response-surface method based on the transfer function to minimize the error derivatives of the chiller system. Results of the proposed method show a robust performance in keeping the PCM temperatures and bacterial-growth value stabilized, allowing a less drastic control compared to the cascade-model predictive control

Keywords: phase-change material, chiller, pasteurization, Smith predictor, RSM tuner

Predstavljena raziskava obravnava uglaševanje shranjevanja latentne toplote fazne spremembe materiala (PCM; angl..: Phase Change of Material) z enkapsuliranimi večstenskimi ogljikovimi nano cevčicami (MWCNT; Multi-wall Carbon Nano Tubes) za hladilni sistem, v procesu pasterizacije mleka z uporabo modela za napoved, ki temelji na metodologiji površinskega odgovora (RSM; angl..: Response Surface Methodology) in uporabi majhnega nadzornega sistema. PCM so sintetizirali z uporabo natrijevega poliakrilata in delcev MWCNT, ki so jih enkapsulirali v krogličnem mlinu, shranjenem v IBT hladilni enoti (IBT; angl.: ice bank tank). Eksperimentalno delo je obsegalo ugotavljanje karakteristik prenosa toplote hladilne enote s pomočjo kontrole pretoka z uporabo servo ventilov, temelječ na centralnem kompozitnem dizajnu eksperimentov. Kaskadni sistem je uporabljal proporcionalno-integralno-diferencualne (PID) krmilnike s Smithovim napovednikom za stabilizacijo latentne toplote med ohlajanjem mleka v hladilnem sistemu. Avtorji so predpostavili, da dvig in čas posedanja potekata po zakonu prvega reda. Dobili so osnovni model z uporabo metode površinskega odgovora, ki temelji na funkciji prenosa, ta pa zmanjšuje diferencialne napake hladilnega sistema. Rezultati predlagane metode so pokazali njeno robustnost pri ohranjanju PCM temperature in stabiliziranju vrednosti rasti (razvoja) bakterij, kar zahteva manj drastične kontrolne ukrepe v primerjavi s kaskadnim modelom kontrole napovedi.

Ključne besede: fazne spremembe materiala, hladilo, pasterizacija, Smithov napovednik, metodologija površinskega odgovora, RSM tuner (uglaševalo)

## 1 INTRODUCTION

Milk is lacteal secretion that is almost completely devoid of colostrum. It is fouled from soiled bedding, manure, feed, milking equipment and milk handlers, invariably resulting in an introduction of psychrotrophic and mesophillic bacteria in large quantities. To increase the shelf life of bovine milk, thermal treatment with three generic techniques has been evolved in dairy industries.[1]

Thermization, sterilization and pasteurization techniques have been utilized to eliminate and control the bacterial growth arising from pathogenic microbial organisms and to minimize the chemical, physical and organoleptic changes that occur in milk during heating. Pasteurization is a nonlinear and multivariable interacting process of heating raw milk from 6 °C to 70 °C, holding it for a period of 15 s in a holding tube and cooling it down to 2–4 °C depending upon the set point in the controller.[2] Since the temperature profiles for milk and water oscillate over the plant requirements, it is challenging to regulate this system using conventional on-off controllers.[3] To ensure that the process parameters are in a steady state, the controller's main objective has to be designed accordingly. Any variation can result in contamination as well as product recall and loss. The pasteurization unit's control mechanism operates as a closed loop system.[4] Its purpose is to keep the temperature of the holding tank outflow close to the process set point. The unit is controlled by a solenoid valve in the passive control process. Modern systems use servo-controlled

---

*Corresponding author's e-mail:
saranyaasn@gmail.com (Saranya Subbiah Natarajan)

valves to adjust both the flow and temperature. Traditional on-off controllers[5] are used to regulate the chiller's water temperature and the ripple plate's temperature. Water and milk temperature profiles fluctuate about the appropriate set points despite the on-off controller's good control performance. Unexpected-movement control actions are also common. They resulted in pasteurized-milk factories consuming insufficient energy.[6] Nonlinear dynamic behaviour including multi-variable interactions between controlled and manipulated variables, and limitations on manipulated and state variables are among the numerous serious control problems that the milk-pasteurisation process poses.[7] PID regulators calibrated using trial and experience should be used to tune a dynamic system with various responses.[8] An in-depth analysis is required before the hunt for better algorithms can begin. In the academic literature, a variety of control approaches and algorithms that can manage portions of the aforementioned problems were published.

Cascade standard PID (proportional-integral-derivative) controllers were designed to optimize the changes in the milk temperature affected by disturbances like milk inlet temperature, flow rate, hot-water temperature and flow rate.[9,10] Pasteurization is nonlinear, and linear control techniques do not work for it according to E. D. J. Rasmussen et al.[11] For a simple PI controller, a simple adaptive algorithm based on the observer-based control was proposed and implemented. In order to verify the control approach, a variety of circumstances were simulated, including time-varying disturbances. In contrast to PI or PID controllers, adaptive rules reduce variance. Any control algorithm's effectiveness is determined on how well it is tuned. According to the literature,[12] a typical PID algorithm can be tuned in both open and closed loop. A good linear model for the system is found and then pre-determined relationships are applied to provide appropriate controller settings. As things progressed, researchers focused on tuning the PID control, including self-tuning and auto-tuning,[13] genetic tuning of PID,[14] robust and optimal tuning[15] and others. Intelligent PID and PID-based control strategies are also discussed as well as fuzzy PID,[16] optimal PID controller design in adaptive PID control[17] and fractional order PID.[18]

RSM is a statistical approach developed by Box and Wilson in 1951.[19] Engineers, biologists and social scientists can all benefit from this method.[20] This method optimises responses by characterising them as a function of design variables. Controller performance is determined by controller responsiveness, but controller tuning parameters are determined by design considerations. To determine the response surface, step-test spanning of controller tuning settings would be required, as well as monitoring the controller performance at each of these points. This information can be utilized to build a controller performance model that is dependent on tuning parameters. This model would also demonstrate how tuning parameters can be intelligently changed into a more profit-generating area. Thermal energy storage, in addition to the employment of the aforementioned management mechanisms, plays a vital part in the storage and dispersion of heat over the required sources. Cold TES systems are also commonly utilised in a variety of industrial applications, such as food storage, where the systems experience significant heat increases.[21] This form of control is effective in managing energy-efficient systems (a pasteurization process). Cool thermal storage systems have been thoroughly investigated for their ability to efficiently utilise stored cooling produced during peak hours to supply the energy required for the proposed applications. In general, there are two basic strategies for storing cold thermal energy: sensible heat and latent heat of phase changes. The chilled-water sensible-heat storage idea, with or without thermal stratification, is a well-developed technique that is reasonably simple. Homan and Soo presented a model of the transient stratified flow into a chilled-water tank.[22] Their paper presents numerical solutions for the transient-flow field with a single jet of cold liquid entering horizontally at the bottom of a tall tank initially filled with hotter liquid removed at the top of the tank. Ismail et al. presented a two-dimensional model for a stratified storage tank based upon the continuity, momentum and energy equations with the Boussinesque approximation as the coupling condition.[23] Silver et al. developed mathematical models for the components of ice banks with the objectives to simulate the thermal performance of such equipment, perform a complete energy analysis and test the control strategies.[24] Berglund presented details of ice banks and showed their importance for thermal control and comfort.[25]

When heated at a given temperature, LHTES causes the storage medium to shift from one state to another, a liquid to a solid or a liquid to a gas. The solid-liquid transition is the most widely used in latent-heat storage applications due to its better efficiency compared to the other transformations. The substance used to store latent thermal energy is known as a phase-change material (PCM). PCMs are available in a wide range of organic, inorganic and eutectic forms, also including a wide range of melting and freezing points. As different materials have varied characteristic qualities, the choice of the material for the latent-heat storage is dependent on the application. The thermal instability at high temperatures, supercooling and phase segregation are other issues relating to PCMs, particularly hydrated-salt PCMs. An introduction of carbonaceous elements as nano-additives into PCMs stabilises the LH storage, overcoming this instability. To stabilise the supercooling effects in an IBT storage, nano-additives such as graphene, $MoS_2$, MWCNT and others were utilised as encapsulating materials.[26] As a result of the aforesaid benefits of a PCM in a chiller-system ice-bank tank, the proposed research focuses on the usage of a nano-added PCM in the IBT of a

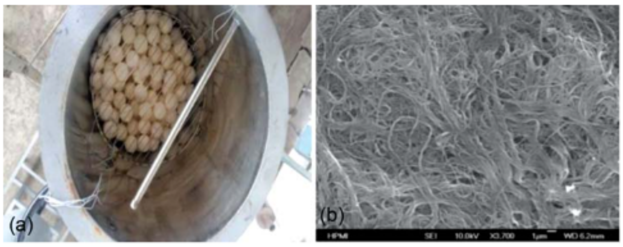

**Figure 1:** a) Photographic image of the PCM in the IBT, b) SEM image of MWCNT particles in sodium polyacrylate

chiller system in the pasteurisation process with an IMC-Smith controller calibrated by RSM.

## 2 MATERIALS AND METHODS

### *2.1 Phase-change materials*

MWCNTs and sodium polyacrylate were ultrasonicated using a 3/4" Qsonica Solid Tip Sonicator Model 334 on a hot plate set to 100 °C to produce a PCM. Sonication allows shifts in amplitude, timing and temperature. Sonication is the employment of high-frequency sound waves to produce a desired effect. Consequently, the combination becomes hotter. Paraffin vaporization makes it imperative that the combination does not exceed 370 °C. This would result in a wax-to-CNT ratio being different from that of the mixed sample. As a result, a comparative analysis would be more variable, which is undesirable. When sonication is completed, the sample-preparation phase begins. Samples must be inspected under a scanning electron microscope (SEM), as illustrated in **Figure 1b**, in order to detect the microstructure. The results show that MWCNT particles are uniformly dispersed in the sodium polyacrylate phase. Using a hot filling injector, the mixture was encased in spherical balls constructed of HDPE. **Figure 1a** depicts a photographic image of the IBT with PCM balls.

### *2.2 Process model*

Using first-order differential equations, the chiller system with a milk flow was described within the process model. These equations are based on the mass and energy balance of each unit. The assumptions used in the model were as follows:

Milk outlet of the plate HX (heat exchanger)

$$\frac{\mathrm{d}T_{\mathrm{mo}}}{\mathrm{d}t}=\frac{F_{\mathrm{m}}(T_{\mathrm{mi}}-T_{\mathrm{mo}})}{V_{\mathrm{pp},i}}\pm\frac{U_{\mathrm{pp},i}A_{\mathrm{pp},i}T_i}{\rho_{\mathrm{m}}c_{\mathrm{ph}}V_{\mathrm{pp},i}} \tag{1}$$

Iced HTF inlet of the IBT

$$\frac{\mathrm{d}T_{\mathrm{ii}}}{\mathrm{d}t}=\frac{u_2F_{\mathrm{m}}(T_{\mathrm{mi}}-T_{\mathrm{mo}})}{V_{\mathrm{pp},4}}\pm\frac{U_{\mathrm{pp},4}A_{\mathrm{pp},4}T_4}{\rho_{\mathrm{m}}c_{\mathrm{ph}}V_{\mathrm{pp},4}} \tag{2}$$

HTF in the IBT

$$\frac{\partial T_{\mathrm{htf}}}{\partial t}=-\left[\frac{c_{\mathrm{htf}}\dot{m}_{\mathrm{htf}}}{A_{\mathrm{htf}}}\frac{\partial T_{\mathrm{htf}}}{\partial x}+A\frac{h_{\mathrm{A}}\pi D_i}{c_{\mathrm{htf}}}(T_{\mathrm{w}}-T_{\mathrm{htf}})\right]\times \\ \times\frac{1}{\rho_{\mathrm{htf}}c_{\mathrm{htf}}} \tag{3}$$

PCM near the IBT wall

$$\frac{\partial H_{\mathrm{pcm}}}{\partial t}=\left[\frac{1}{s_{\mathrm{w}}}\left(\frac{k_{\mathrm{w}}A^{1}_{\mathrm{pcm}}}{A_{\mathrm{w}}}+\frac{k_{\mathrm{pcm}}A^{1}_{\mathrm{pcm}}}{A_{\mathrm{w}}}\right)(T_{\mathrm{pcm}}-T_{\mathrm{w}})+\right. \\ \left.+\frac{1}{s_{\mathrm{w}}}\frac{k_{\mathrm{pcm}}}{A_{\mathrm{pcm}}}\left(\frac{H^{j+1}_{\mathrm{pcm}}}{A_{\mathrm{w}}}-\frac{A^{j}_{\mathrm{pcm}}}{A_{\mathrm{w}}}\right)\right]\times\frac{1}{\rho_{\mathrm{pcm}}} \tag{4}$$

PCM sequential to the PCM near the wall

$$\frac{\partial H_{\mathrm{pcm}}}{\partial t}=\left\{\frac{k_{\mathrm{pcm}}}{c_{\mathrm{pcm}}}\left[\frac{1}{r}\frac{\partial}{\partial r}\left(r\frac{\partial H_{\mathrm{pcm}}}{\partial r}\right)\right]\right\}\times\frac{1}{\rho_{\mathrm{pcm}}} \tag{5}$$

Iced HTF outlet of the IBT

$$\frac{\mathrm{d}T_{\mathrm{io}}}{\mathrm{d}t}=\frac{u_2F_i(T_{ii}-T_{\mathrm{to}})}{V_{\mathrm{rp}}}+\frac{\pi(u_4n_{\mathrm{s}})d_{\mathrm{f}}h_{\mathrm{fg}}A_{\mathrm{f}}}{60\rho_iC_{\mathrm{p}i}V_{\mathrm{rp}}v}- \\ -\frac{U_{\mathrm{rp}}A_{\mathrm{rp}}(T_{\mathrm{io}}-T_{\alpha})}{\rho_iC_{\mathrm{p}i}V_{\mathrm{rp}}} \tag{6}$$

$A_{\mathrm{pcm}}$, $A_{\mathrm{pp4}}$ – flow area of ripple HX and PCM IBT
$A_{\mathrm{htf}}$ – heat-transfer fluid area in the IBT
$C_{\mathrm{pm}}$, $C_{\mathrm{p}i}$, $C_{\mathrm{htf}}$, $C_{\mathrm{pcm}}$ – specific-heat capacity
$d_{\mathrm{f}}$ – pump diameter
$F_{\mathrm{m}}$ – flow rate of milk
HTF, htf – heat-transfer fluid
$n_{\mathrm{s}}$ – pump-rotation speed
$T_{\mathrm{m}i}$, $T_{\mathrm{mo}}$ – temperature of milk at inlet and outlet
$T_{\mathrm{htf}}$ – temperature of heat-transfer fluid inside the IBT
$\mathrm{T_w}$ – temperature of PCM wakk with interference to htf at IBT
$t$ – time
$u_2$, $u_4$ – manipulated variables
$V_{\mathrm{rp}}$, $V_{\mathrm{ct}}$ – water volume for the ripple plate and cooling towers
$V_{\mathrm{pp4}}$ – fluid volume for PP
$\rho_{\mathrm{m}}$, $\rho_{\mathrm{i}}$, $\rho_{\mathrm{htf}}$ – density of milk, iced water and htf

### *2.3 IMC-Smith control*

As demonstrated in **Figure 2**, the suggested IMC Smith control was designed, using a traditional PID controller with an internal Smith predictor model. The basic Smith-predictor closed-loop transfer function is given as

$$T_{\mathrm{smith}}(s)=\frac{G_{\mathrm{c}}(s)G_{\mathrm{m}}(s)e^{-\mathrm{L}ms}}{1+G_{\mathrm{c}}(s)G_{\mathrm{m}}(s)} \tag{7}$$

It is necessary to formulate the transfer function of the internal model control using the Smith predictor as

$$T_{\mathrm{IMC}}(s)=G_{\mathrm{IMC}}(s)G(s)e^{-\mathrm{L}s} \tag{8}$$

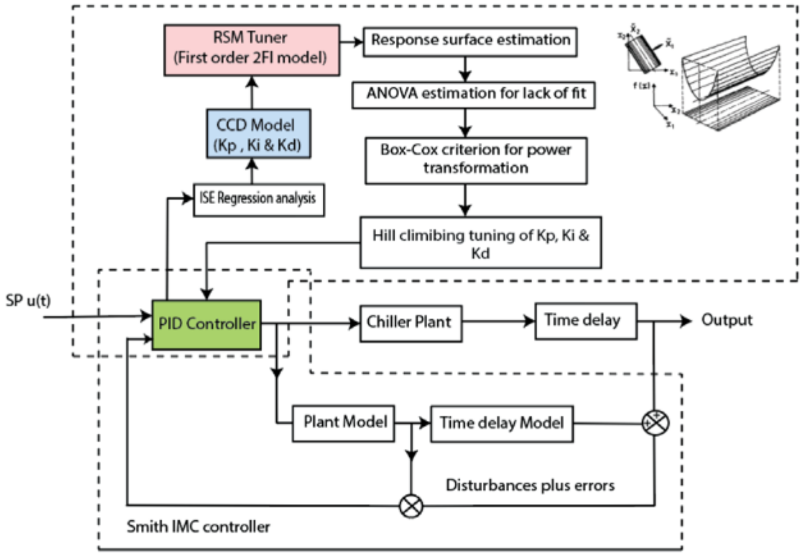

**Figure 2:** Architecture of the RSM auto-tuning-based Smith controller

where $G_m(s)$ is the delay-free part of the model transfer function. In order to demonstrate that the IMC controller has the same output for both configurations, comparing the above equations is a convenient way to illustrate that $G_{IMC}(s)$ is related to the classical controller $G_c(s)$ through the transformation

$$G_{IMC}(s) = \frac{G_c(s)}{1+G_c(s)G_m(s)} \tag{9}$$

The process model must be formulated with the stated equation in order to obtain the IMC controller.

$$\widetilde{G} = \frac{K_m e^{-Lms}}{T_m s+1} \tag{10}$$

The following equations are found using a first-order Taylor series expansion for the time-delay approximation.

$$\widetilde{G}_+(s) = (1-Ls) \tag{11}$$

$$\widetilde{G}_-(s) = \frac{K_m}{T_m s+1} \tag{12}$$

The IMC controller can be obtained as follows:

$$G_{IMC}(s) = \frac{T_m s+1}{K_m(\lambda s+1)} \tag{13}$$

Once the model parameters, $K_m$ and $T_m$, are known, filter parameter $\lambda$ needs to be chosen. The classical PID controller, $G_c(s)$, can then be obtained as

$$G_c(s) = \frac{T_m s+1}{K_m \lambda s)} \tag{14}$$

Following the same procedure as for the first-order process delay time transfer function and assuming that

$$\widetilde{G}_-(s) = \frac{K_m e^{-L_m s}}{(T_{1m}s+1)(T_{2m}s+1)} \tag{15}$$

It can easily be illustrated that the classical controller may now be implemented as a PID controller using the parameters shown below.

$$K_p = \frac{T_{1m}+T_{2m}}{K_m L_m} \tag{16}$$

$$K_i = T_{1m}+T_{2m} \tag{17}$$

$$K_d = \frac{T_{1m}T_{2m}}{T_{1m}+T_{2m}} \tag{18}$$

### 2.4 RSM-based auto tuner

**Table 1:** Coded factors for the combination of $K_p$, $K_i$ and $K_d$ using a central composite design

| Std | A: $Kp$ | B: $K_i$ | C: $K_d$ | ISE (Error values) |
|---|---|---|---|---|
| 14 | 6.7736 | 1385.665 | 387.74 | 50.956 |
| 17 | 6.7736 | 1385.665 | 285.015 | 42.874 |
| 13 | 6.7736 | 1385.665 | 182.28 | 16.528 |
| 20 | 6.7736 | 1385.665 | 285.015 | 38.467 |
| 11 | 6.7736 | 930.68 | 285.015 | 12.632 |
| 19 | 6.7736 | 1385.665 | 285.015 | 14.765 |
| 16 | 6.7736 | 1385.665 | 285.015 | 17.747 |
| 8 | 13.14 | 814.61 | 570.46 | 24.138 |
| 4 | 13.14 | 2000.0 | 132.72 | 14.842 |
| 5 | 1.06 | 814.61 | 570.46 | 15.135 |
| 3 | 1.06 | 2000.0 | 132.72 | 7.05 |
| 15 | 6.7736 | 1385.665 | 285.015 | 22.482 |
| 6 | 13.14 | 814.61 | 570.46 | 28.742 |
| 2 | 13.14 | 814.61 | 132.72 | 35.427 |
| 12 | 6.7736 | 1840.65 | 285.015 | 11.724 |
| 18 | 6.7736 | 1385.665 | 285.015 | 30.182 |
| 9 | 3.0722 | 1385.665 | 285.015 | 44.821 |
| 1 | 1.06 | 814.61 | 132.72 | 42.342 |
| 7 | 1.06 | 2000.0 | 570.46 | 47.821 |
| 10 | 10.475 | 1385.665 | 285.015 | 28.428 |

**Figure 2** shows a block diagram for the IMC-Smith predictor configuration's auto tuning. The response-surface method is used to construct the tuning functions for PID controllers, considering single-valued measures of the controller performance such as IAE (integral absolute error), ITAE (integral time-weighted absolute error) and ISE (integral squared error). In order to select the tuning, one must first select ISE, IAE or ITAE. As a result of minimising ISE, performances will have minimal overshoots but will be oscillatory in character. ITAE is weighted highly in terms of late-in-time errors but is insensitive to the initial, often unavoidable, error, whereas IAE is more sensitive to smaller errors than larger ones.[27] The noise in the process response also affects these metrics. A good controller should be able to quantify the tuning while being somewhat insensitive to disturbances in the measurement of a process. The chiller plant was operated for a total of 15 min in our proposed task. With the help of the controller, the process reached its steady-state value after 5 min; nevertheless, the value of ITAE for 15 min was only 70 % of its ultimate value, while ISE amounted to 99.3 % of its final value. As a result, the effect of noise, not the tuning parameters, increased the value of ITAE. Hence, the effect of noise, and not the tuning settings, raised the value of ITAE. Due to the fact that the ISE criterion is less sensitive to noise, it is more suitable for our purposes than the ITAE criteria.

The first order process based delay-time transfer function is studied with ISE to determine the tuning parameters for the controller $Gc(s)$ with the response-surface methodology. The integral-squared-error criterion, or ISE, is used here.

$$J_{ISE} = \int_0^\infty \left[r - c(t)\right]^2 \,\mathrm{d}t \tag{19}$$

The major goal of the proposed system is to reduce the ISE by using PID tuning for a unit set-point change. Although minimising ISE produces oscillatory responses for set-point changes,[28] it is widely employed in practise. However, RSM might be used to fine-tune the three control parameters $K_p$, $K_i$ and $K_d$ for the first-order design in a systematic way. A set-point change was applied to each experimental setting of $K_p$, $K_i$ and $K_d$, and the ISE was calculated from the process response. Using the central composite design of experiments (**Table 1**), all runs were conducted. As indicated in **Table 2**, a first-order model was employed to fit the data with ANOVA response. Tests were conducted to determine if the model fit correctly and if there was any surface curvature.[28] From **Table 2**, the F-value for the present model is found to be 5.01, which is less than the F-critical value observed on the F-table. This denotes that the model is significant, with $\alpha = 0.05$. The p-value is found to be less than 0.05, proving the model significance. These two parameters are important for describing the model significance. The F-value describes the variations in the oscillations based on the setpoint value. If the oscillations are high for the first-order model, then the F-value becomes higher than the F-critical value, rejecting the model. Likewise, if the p-value is found to be higher than 0.05, the model is consistent, therefore suitable for tuning. So, before obtaining the tuning parameters, the F-value and p-value are calculated based on the ANOVA method to find the model significance required for effective tuning.

For the use of the central composite design, the upper and lower limits of $K_p$, $K_i$ and $K_d$ were assumed based on the Zeiger-Nicholas method, obtaining the initial assumption from adaptive tuning. With these limits, the design is framed with the calculated ISE, as shown in **Table 1**. The response-surface contours of these tuning parameters with the impact on the ISE values are displayed in **Figure 3**. This contour plot defines the response prediction for combination inputs of $K_p$, $K_i$ and $K_d$ to find the maximum impact on the ISE. The regression model for the response function of the ISE was developed as follows:

$$\begin{aligned}\mathrm{ISE} = {} & 106.93 - 14.14 \cdot K_p - 0.164 \cdot K_i + 0.069593\,K_d \\ & + 0.019122\,K_p \cdot K_i - 0.015133\,K_p \cdot K_d\end{aligned} \tag{20}$$

For each experiment, these methods resulted in a distribution of ISE measurements. The ANOVA response for the suggested BBD model is shown in **Table 2**. For

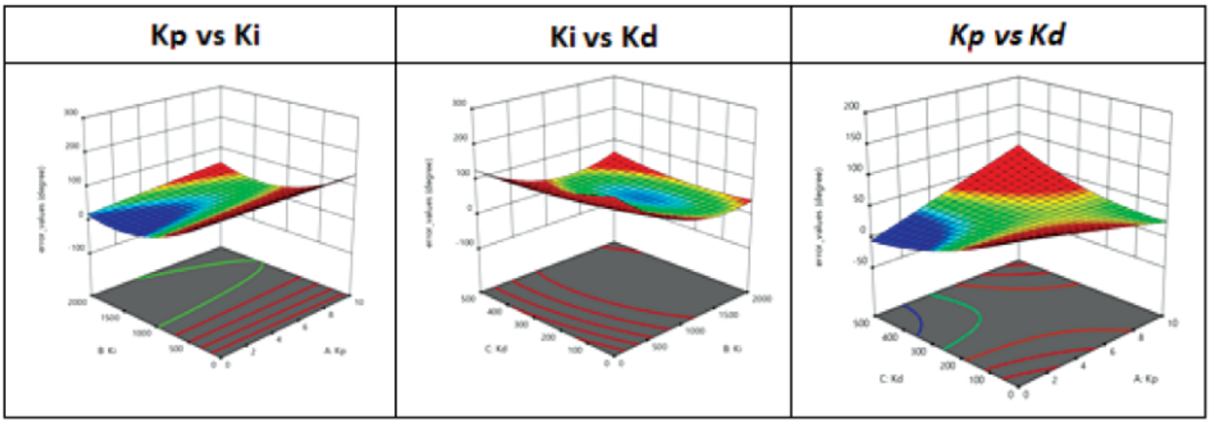

Figure 3: Model interaction plots for $K_p$, $K_i$ and $K_d$ for the valve control

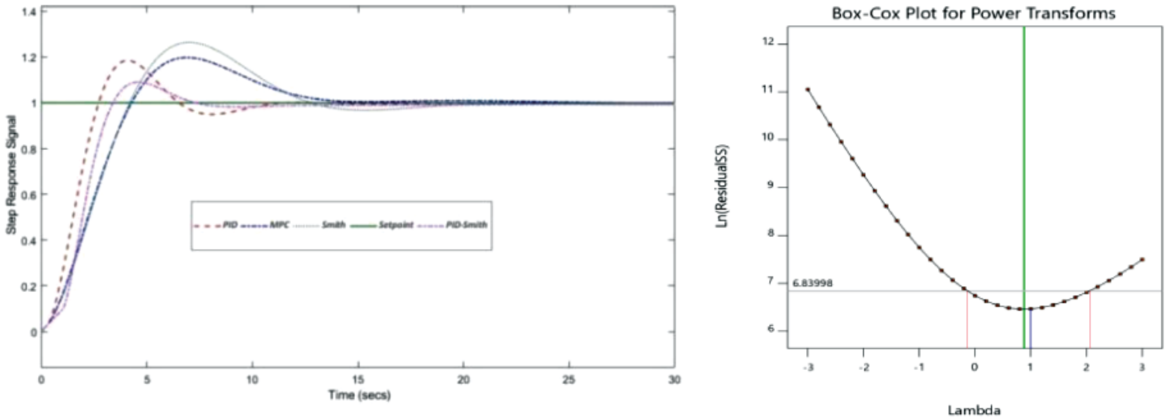

**Figure 4:** a) Tuning response of a step signal, b) Box-Cox plot for the convergence-value criterion

the first-order steepest ascent strategy, the 2FI model was chosen. The corrected coefficient of determination, R2, for the model was 0.818, indicating that the model explains 81.8 % of the variations in the data when the degrees of freedom are taken into account. A test of surface curvature indicated a considerable amount of curvature of the surface. **Figure 4** shows the tuning response of the step signal with the reduction in the oscillations for PID, MPC and IMC-Smith control. The tuning response is found to be minimal with a lesser amount of overshoots and no oscillation was observed. Regarding power transforms, the Box-Cox plot presented in **Figure 4b** shows the statistical intervals based on normality. Defining the normality of the real set of data in a transform function, we use Box-Cox transformation $Y\lambda$, where $\lambda$ is between –0.2 and 2. Finding the value of that minimizes the variation is the purpose of this procedure (standard deviation). The $\lambda$ value is set to 0.8, which is the default. The current transformation is depicted in blue. It points to a value of 1 for $\lambda$ in this case, which represents the power applied to the response values. The $\lambda$ value of 1 denotes that no transformation has occurred. The best $\lambda$ value is indicated by the green line. As shown in **Figure 4b**, the blue line falls within the green line, predicting data in the optimal zone, therefore no changes to the response transformation are required.

**Table 2:** ANOVA table for the first-order 2FI model

| Source | df | Mean square | F-value | p-value | |
|---|---|---|---|---|---|
| Model | 9 | 320.85 | 5.01 | 0.0095 | significant |
| A – $K_p$ | 1 | 336.60 | 5.26 | 0.0447 | |
| B – $K_i$ | 1 | 184.09 | 2.88 | 0.1207 | |
| C – $K_d$ | 1 | 1.01 | 0.0158 | 0.9023 | |
| AB | 1 | 192.25 | 3.00 | 0.1137 | |
| AC | 1 | 301.32 | 4.71 | 0.0552 | |
| BC | 1 | 27.57 | 0.4310 | 0.5263 | |
| Residual | 10 | 63.98 | | | |
| Cor. total | 19 | | | | |
| Std. dev. | 8.00 | | $R^2$ | 0.8186 | |
| Mean | 27.36 | | Adjusted $R^2$ | 0.6554 | |

## 2.5 Experimental work

Experimental work was conducted using the process parameters shown in **Table 3**. The dynamic response time output was recorded using a data-acquisition system (HANTEK 8 channel DAQ) with RTD sensors located at the zones of measurements, as shown in **Figure 5**.

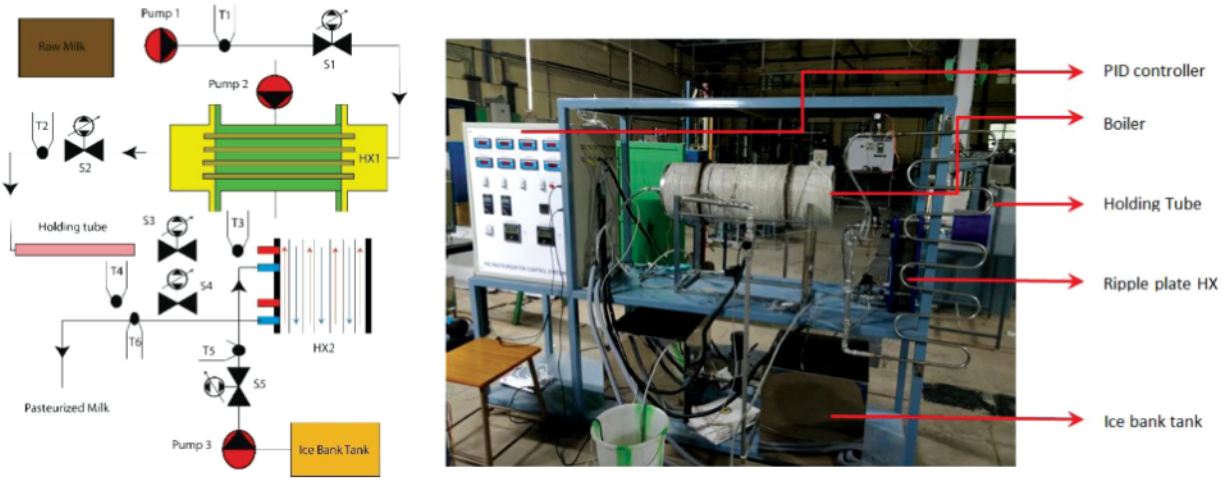

**Figure 5:** Schematic diagram and photography of the proposed pasteurization process

**Table 3:** Process parameters and their levels

| Milk | Heat-transfer fluid | RTD probe | Flow sensor | | | | |
|---|---|---|---|---|---|---|---|
| Heat-transfer volume (m$^3$) | 0.00679 | Cold-water volume (m$^3$) | 0.18 | type | PT100 | type | Hall effect |
| $V_{pp4}$ (m$^3$) | 0.02 | | | | | range | 0–130 L/min |
| $F_m$ (m$^3$/s) | 0.0127 | Cold-water temperature | 281.15 K | range | –200 °C to 850 °C | sensitivity | 0.5 V ± 0.1 V |
| overall heat-transfer coefficient (W/m$^2$·K) | 0.002 | | | sensitivity | 0.1 °C to 1 °C | output | digital |
| Microcontroller | Servo valve | RPHE (Hx) | PCM [Sodium polyacrylate and MWCNT] (IBT) | | | | |
| type | AT MEGA 2560 | type | ball valve | type | gasket | melting point | 16–18 °C |
| BIT | 32 bit | accuracy | 1.8° | no. of plates | 30 | freezing point | 8 °C |
| | | | | | | latent heat of PCM | 143.2 J/kg |
| analog inputs | 14 channels | sensitivity | 5 ms | convective heat-transfer coefficient (W/m$^2$K) | 50 | density of solid state PCM $\rho_s$ | 924 kg/m$^3$ |
| | | | | | | thermal conductivity (liquid) | 2.8 W/m·K at 71 °C |
| programmer | matlab | fully open at degrees | 0° | cooling efficiency (%) | 0.75 | thermal conductivity (solid) | 1.3 W/m·K at 30 °C |

A servo-operated gate valve was used to control the flow rate of the milk at the entry and exit of the zones. The process was conducted for a time of 30 min, of which 15 min was taken to maintain the steady state with the aid of a classical PID controller. In order to minimize the time taken for the steady state response, the proposed IMC-Smith controller was used. This controller was operated based on the response outputs obtained from the classical controller as a process with a time delay. The process model was obtained based on the equations provided for the section with the time-delay function. The error states were tuned using the RSM tuner based on the minimization of the ISE value. The response-control outputs of the temperature and valve angle were compared with the classical PID and Smith controllers.

## 3 RESULTS AND DISCUSSIONS

The main purpose of this simulation study is to evaluate the control performance of the RSM-tuned IMC Smith control compared to the MPC and classical PID approach. Here, the IMC-Smith algorithm was studied to keep the milk temperature at the plate heat exhanger ($T_{mo}$) to the plant's requirements, as well as the iced-water temperature $T_{io}$ to the desired set points. These are controlled by adjusting the milk and iced water flow rate at the PP ($u_{milk}$ and $u_2$) through the servo/proportional control valves.

The "charging time vs. temperature" of the PCM balls in the IBT is shown in **Figure 6** for the variations in the tank height of T1 = 30 mm, T2 = 60 mm, T3 = 70 mm, T4 = 80 mm and T5 = 100 mm. All the legends were plotted for the constant value of the HTF flow rate inside the IBT of 2 L/min, inlet HTF temperature of 40 °C, and effective thermal conductivity of 2.8 W·m$^{-1}$·K$^{-1}$. The variation in the height of the PCM balls influences the convective surface area of the balls, their porosity and the maximum value of the internal conductive resistance. It was noted that the charging temperature decreased at a time of 100 min, while a faster charging rate was observed for T1 at the base layer of the IBT, which absorbs the sensible heat of conduction and reaches the sub-zero state in 25 min. A slow rate of charging the HTF was observed for T5, which only absorbs the latent heat from the preceding layers in a concentric manner towards the sectional layer of the PCM balls and then towards the adjacent layer. It was also noted that for a given increase in the height of the ball placement in the IBT, there is a proportionate uniform increase in the charging time at all heights of the storage tank.[29] The charging temperature of the base PCM balls was –8 °C. The system achieved its steady state temperature in 25 min, with the maximum drop in the charging temperature (–2 °C to 10 °C).

The data recorded from the controller involves the set-point tracking and a model mismatch case based on

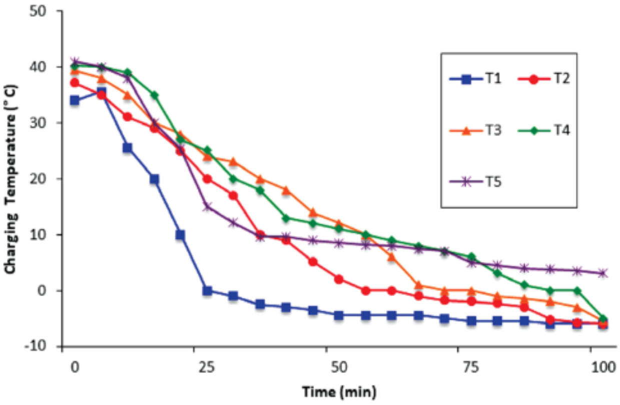

**Figure 6:** Variations of HTF temperature during the charging process at different IBT heights at a flow rate of 2 L/min

**Table 4:** Point prediction and confirmation location of MPC and RMS-PID control

| Zones | $K_p$ | | | | $K_i$ | | $K_d$ | |
|---|---|---|---|---|---|---|---|---|
| | MPC | | RMS-PID | | MPC | RMS-PID | MPC | RMS-PID |
| Output $T_{mo}$ | 15.47 | | 1.20908 | | 64.23 | 500 | 82.69 | 100.001 |
| Error values | Predicted mean | | Predicted median | | Std. dev. | | F-value | |
| | MPC | RMS-PID | MPC | RMS-PID | MPC | RMS-PID | MPC | RMS-PID |
| Valve $T_{mo}$ | 75.68 | 15.1768 | 954.23 | 15.1768 | 101.56 | 7.99885 | 356.21 | 12.3194 |

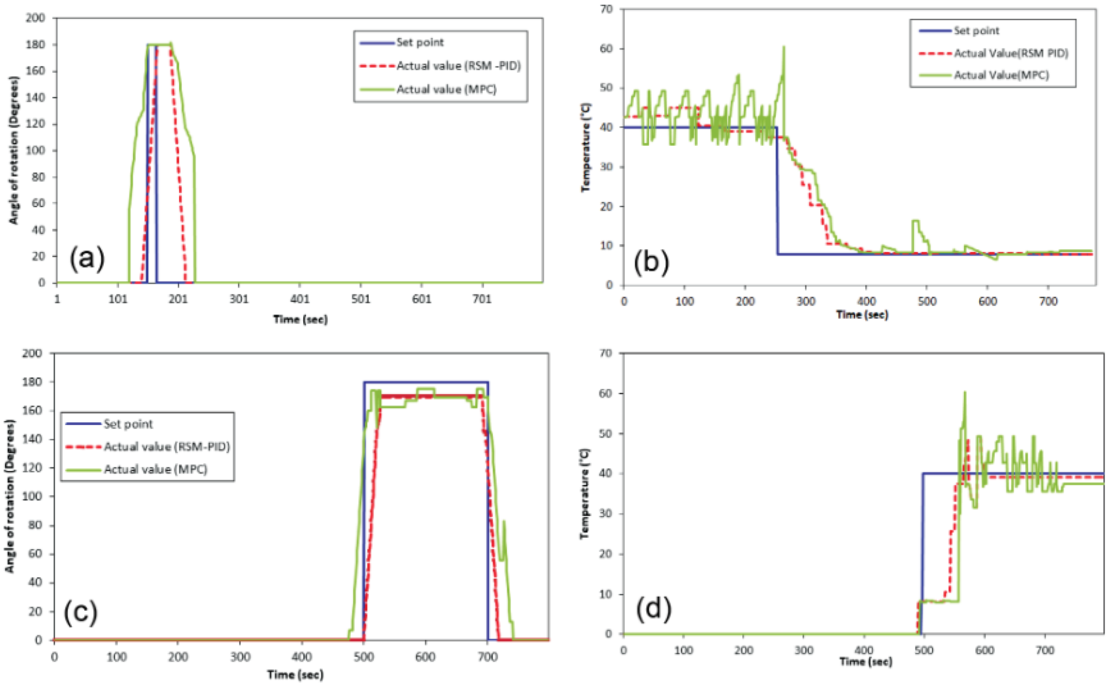

**Figure 7:** Set point and control response of MPC and RSM-PID controller for the plate heat exchanger: a) valve O/C, b) outlet temperature vs. process time and IBT, c) valve O/C, d) outlet temperature vs. process time

the first-order transformation with overshoots and settling time. **Figure 7** shows the set point and control response of the plate heat exchanger for the MPC and RSM-Smith controller. It was noted that **Figure 7a** shows the response of the valve angle that defines the flow rate of milk with a minimum increase to 105 min and settling time of 205 min for the RSM smith controller. The error difference between the MPC and RSM-Smith controllers was found to be 7 min for the rise time and 4 min for the settling time. **Figure 7b** shows the response of the temperature with higher oscillations observed in the setpoint zone for MPC, increasing the order of the model to tune. The oscillations were due to ineffective tuning capabilities of MPC in comparison to the RSM-Smith controller that was found to reach the set point time in 250 min. As for the set point tracking case, MPC is designed to bring the milk temperature as well as the iced-water temperature to the desired set points from the initial values. The desired points of the temperature are set at –8 °C for the cooling stage and 2 °C for the ripple plate. **Figure 7c** shows the response of the valve angle at the IBT, which determines the charge of PCM balls. The temperature response of the HTF in the IBT with second-order oscillations from **Figure 7d** was found with the MPC controller. The proposed RSM-PID controller reduces the number of oscillations, keeping the ones with only a single overshoot in a shorter period of the settling time. The effective point prediction of the RSM tuner for $K_p = 1.209$, $K_i = 500$ and $K_d = 100$ included the mean of the ISE error, which was 15.17. In comparison, with MPC, the error value was 75.68, creating a drastic difference in optimistic tuning.

## 4 CONCLUSIONS

From the above discussions of tuning the output milk temperature from the plate heat exchanger with the PCM-based chiller unit and RSM-tuned IMC-Smith controller, the following conclusions were drawn. The RSM tuner reduces the undamped oscillations obtained through the latent-heat transfer of milk in the plate heat exchanger and the PCM in the IBT with a first-order 2FI model. In comparison with the classical PID and MPC, the proposed RSM IMC-Smith reaches the set point in a shorter time without oscillations and overshoots. The factors of tuning through the statistical response surface approach provide for a novel strategy of reducing the ISE error rates with an optimum selection of $K_p$, $K_i$ and $K_d$ that stabilizes the valve control and output temperature in the IBT and plate heat exchanger. In comparison with the other controllers like PID and MPC, the proposed model gave better results with respect to process disturbances and time delay by tuning the parameters for the controller based on the design obtained with the experimental approach. Future steps could be taken in the development of the process model using metaheuristic approaches and signal-processing filters that can reduce the undamped oscillations of the real-time plant model. This could simplify the tuning efforts, providing stable and robust control of the pasteurization process.

## 5 REFERENCES

[1] E. T. Ryser, Encyclopedia of Dairy Sciences, 2nd Edition, Elsevier, 2011, 310–315, doi:10.1016/b978-0-08-100596-5.21367-x

[2] V. K. Mishra, L. Ramchandaran, Emerging Dairy Processing Technologies: Opportunities for the Dairy Industry, 1st Edition, John Wiley & Sons, New Jersey 2015, 33–70, doi:10.1002/9781118560471.ch2

[3] S. Niamsuwan, P. Kittisupakorn, I. M. Mujtaba, Predictive Control Strategy for Temperature Control for Milk Pasteurization Process, Proceedings of the 23rd European Symposium on Computer Aided Process Engineering – ESCAPE 23, 2013, 109–114, doi:10.1016/b978-0-444-63234-0.50019-1

[4] M. Indumathy, S. Sobana, R. C. Panda, Identification of high temperature short time milk pasteurization unit, Journal of Food Process Engineering, 43 (**2020**) 7, 1–13, doi:10.1111/jfpe.13410

[5] J. J. Ibarrola, J. C. Guillén, J. M. Sandoval, M. García-Sanz, Modelling of a high temperature short time pasteurization process, Food Control, 9 (**1998**) 5, 267–277, doi:10.1016/s0956-7135(98)00016-4

[6] J. J. Ibarrola, J. M.Sandoval, M. Garci´a-Sanz, M. Pinzolas, Predictive control of a high temperature–short time pasteurisation process, Control Engineering Practice, 10 (**2002**) 7, 713–725, doi:10.1016/S0967-0661(02)00029-1

[7] S. Niamsuwan, P. Kittisupakorn, M. Iqbal Mujtaba, Optimization approach to minimize energy consumption in pasteurized milk process, 2011 International Conference on Chemistry and Chemical Process, IPCBEE, 10 (**2011**), 35–39

[8] S. Bucz, A. Kozakova, PID Control for Industrial Processes, 2018, 73–119, doi:10.5772/intechopen.76069

[9] K. R. Morison, Steady-state control of plate pasteurisers, Food Control, 16 (**2005**) 1, 23–30, doi:10.1016/j.foodcont.2003.11.001

[10] A. Negiz, A. Cinar, J. E. Schlesser, P. Ramanauskas, D. J. Armstrong, W. Stroup, Automated control of temperature short time pasteurization, Food Control, 7 (**1996**) 6, 309–315, doi:10.1016/S0956-7135(96)00048-5

[11] E. D. J. Rasmussen, M. Errico, S. Tronci, Adaptive Feedback Control for a Pasteurization Process, Processes, 8 (**2020**) 8, 930, doi:10.3390/pr8080930//scw

[12] W. K. Ho, O. P. Gan, E. B. Tay, E. L. Ang, Performance and gain and phase margins of well-known PID tuning formulas, IEEE Transactions on Control Systems Technology, 4 (**1996**) 4, 473–477, doi:10.1109/87.508897

[13] H. Koivo, J. Tanttu, Tuning of PID conrollers: Survey of SISO and MIMO techniques, IFAC Proceedings Volume, 24 (**1991**), 75–80, doi:10.1016/S1474-6670(17)51299-9

[14] B. Porter, A. H. Jones, Genetic tuning of digital PID controllers, Electronic Letters, 28 (**1992**) 9, 843–844, doi:10.1049/el:19920533

[15] A. N. Gundes, A. B. Ozguler, PID stabilization of MIMO plants, IEEE Transactions on Automatic Control, 52 (**2007**) 8, 1502–1508, doi:10.1109/TAC.2007.902763

[16] C. H. Hsieh, J. H. Chou, Design of optimal PID controllers for pwm feedback systems with bilinear plant, IEEE Transactions on Control Systems Technology, 15 (**2007**) 6, 1075–1079, doi:10.1109/TCST.2007.908084

[17] Y. F Chan, M. Moallem, W. Wang, Design and implementation of modular FPGA-based PID controllers, IEEE Transactions on Industrial Electronics, 54 (**2007**) 4, 1898–1906, doi:10.1109/TIE.2007.898283

[18] K. C. Sio, C. K. Lee, Stability of fuzzy PID controller, IEEE Transactions on Systems, Man, and Cybernetics - Part A: Systems and Humans, 28 (**1998**) 4, 490–495, doi:10.1109/3468.686710

[19] K. J. Astrom, Adaptive feedback control, Proceedings of the IEEE, (**1987**), 185–217, doi:10.1109/proc.1987.13721

[20] M. Reza, A. Nemati, Applications of MATLAB in Science and Engineering, IntechOpen, Poland 2011, doi:10.5772/22657

[21] E. Nakano, A. Jutan, Application of response surface methodology in controller fine-tuning, ISA Transactions, 33 (**1994**) 4, 353–366, doi:10.1016/0019-0578(94)90017-5

[22] K. O. Homan, S. L. Soo, Model for the transient stratification into a chilled-water storage tank, International Journal of Heat Mass Transfer, 40 (**1997**) 18, 4367–4377, doi:10.1016/S0017-9310(97)00063-X

[23] K. A. R. Ismail, J. F. B. Leal, M. A. Zanardi, Models of liquid storage tanks, Energy, 22 (**1997**) 8, 805–815, doi:10.1016/S0360-5442(96)00172-7

[24] S. C. Silver, A. Milbitz, B. D. Hunn, Component models for computer simulation of ice storage tanks, ASHRAE Transactions, 95 (**1989**) 1, 1214–1226

[25] L. G. Berglund, Comfort benefits for summer air conditioning with ice storage, ASHRAE Transactions, 97 (**1991**) 1, 834–847

[26] R. H. Myers, A. I. Khuri, W. H. Carter, Response surface methodology: 1966-1988, Technometrics, 31 (**1989**), 137–157, doi:10.2307/1268813

[27] K. A. R .Ismail, O. C. Quispe, J. R. Henri´quez, A numerical and experimental study on a parallel plate ice bank, Applied Thermal Engineering, 19 (**1999**) 2, 163–193, doi:10.1016/s1359-4311(98)00024-6

[28] S. Sharma, L. Micheli, W. Chang, A. A. Tahir, K. S. Reddy, T. K. Mallick, Nano-enhanced Phase Change Material for thermal management of BICPV, Applied Energy, 208 (**2017**), 719–733, doi:10.1016/j.apenergy.2017.09.076

[29] A. A. Rovira, P. W. Murrill, C. L. Smith, Tuning controllers for setpoint changes, Instrument Control Systems, 42 (**1969**), 67–69